Dalton Transactions

Novel syntheses of carbazole-3,6-dicarboxylate ligands and their utilization for porous coordination cages

Journal:	*Dalton Transactions*
Manuscript ID	DT-ART-03-2020-001149.R1
Article Type:	Paper
Date Submitted by the Author:	12-May-2020
Complete List of Authors:	Rowland, Casey; University of Delaware, Chemistry and Biochemistry Yap, Glenn; University of Delaware, Bloch, Eric; University of Delaware, Chemistry and Biochemistry

ARTICLE

Novel syntheses of carbazole-3,6-dicarboxylate ligands and their utilization for porous coordination cages

Received 00th January 20xx,
Accepted 00th January 20xx

DOI: 10.1039/x0xx00000x

Casey A. Rowland,[a] Glenn P. A. Yap[a] and Eric D. Bloch*,[a]

The molecular nature, and thus potential solubility, of coordination cages endows them with a number of advantages as compared to metal-organic frameworks and other extended network solids. However, their lack of three-dimensional connectivity typically limits their thermal stability as inter-cage interactions in these materials are relatively weak. This is particularly the case for carbazole-based coordination cages. Here, we report the design and synthesis of a benzyl-functionalized octahedral coordination cage that displays moderate surface area and increased thermal stability as compared to its unfunctionalized counterpart. Structural analysis suggests the increased thermal stability is a result of aryl-aryl interactions between ligand groups on adjacent cages. We have further adapted the ligand synthesis strategy to afford a novel, high-yielding preparatory route for the isolation of carbazole-3,6-dicarboxylic acid that does not rely on pyrophoric reagents or transition metal catalysts.

Introduction

Porous metal-organic materials, which can further be broken down into subclasses of metal-organic frameworks (MOFs)[1-6] and porous coordination cages (PCCs, metal-organic polyhedra, metal-organic cages),[7-11] share the distinguishing feature in they are comprised of metal nodes linked together with organic bridging ligands. Similar combinations of metals and ligands can be used to synthesize both classes of materials. However, MOFs are extended two- or three-dimensional materials whereas cages are discrete molecules. Although the former have been more widely studied in terms of their porosity, the molecular nature of cages makes them potentially soluble which can be advantageous in their synthesis,[12] purification,[13] characterization,[14] and utilization.[15] Further, their molecular nature allows for cages to adopt a vast array of structure types that are predictable based on molecular-level design parameters.[16] For example, Zhou and coworkers have shown that for a series of dicarboxylate-based ligands, the ultimate geometry and nuclearity of the cage is determined by the angle between the metal-bonding groups on the ligand.[17] Similarly, Fujita and coworkers have shown that the size of pyridyl ligand-based cages is determined by the angle between binding groups on the organic ligand.[18] Many of the coordination cages that have been prepared have been based on these two types of organic ligand groups, carboxylic acids and pyridines.[19,20,21] However, permanent porosity has only been demonstrated for cages based on the former.

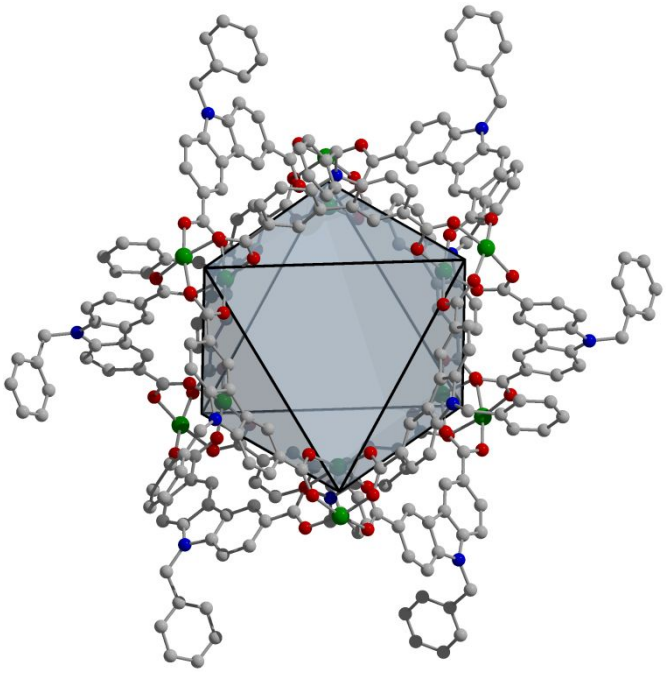

Fig. 1 An octahedral carbazole-based coordination cage, Cu_{12}(benzyl-cdc)$_{12}$ where green, grey, red, and blue atoms represent copper, carbon, oxygen, and nitrogen atoms, respectively. Hydrogen atoms and solvent molecules have been omitted for clarity.

In terms of porous carboxylate-based coordination cages, the octahedral and cuboctahedral structures utilizing carbazoledicarboxylic acid (90° ligand angle, Figure 1) and isophthalic acid (120° ligand angle), respectively, are the most common.[22] While the first isophthalate-based cage Cu_{24}(bdc)$_{24}$ was synthesized in 2001,[23] porosity for these types of cages

[a] Department of Chemistry and Biochemistry, University of Delaware, Newark, Delaware 19716, United States. E-mail: edb@udel.edu

Electronic Supplementary Information (ESI) available: adsorption isotherms, spectroscopic data, crystallographic information. See DOI: 10.1039/x0xx00000x

was discovered significantly later with the synthesis of the functionalized molybdenum-based cage $Mo_{24}(^{t}Bu\text{-}bdc)_{24}$ (SA_{BET} = 437 m^2/g)[24]. In the time since these original reports, isophthalate-based cages with Ni,[25] Cr,[8] Ru,[26] and Rh[27] have also been published and shown to be permanently porous. For a subset of these metals, extensive 5-position ligand functionalization has been reported including triisopropylsilylethynyl,[28] sulfonyl,[23] hydroxyl,[29] alkoxide,[30] amino,[31] and amide groups.[32] Ligand functionalization of these materials endows them with number different properties including tuneable solubility and enhanced thermal stability. The non-functionalized isophthalate-based cages are typically only sparingly soluble in amide solvents such as N,N-dimethylformamide, whereas hydroxyl and alkoxide functionalized cages have shown solubility in methanol, ethanol, tetrahydrofuran, and chloroform. Recently Furukawa, Maspoch, and coworkers showed that modification of metal-bound moieties on $Rh_{24}(OH\text{-}bdc)_{24}$ ($OH\text{-}bdc^{2-}$ = 5-hydroxy-isophthalate) had a significant impact on the solubility of the cage.[14] Enhancement of the solubility of these cages is critical for their incorporation into polymers or other nanoporous materials. Functionalization has also been shown to increase olefin/paraffin selectivity for a subset of these cages.[13]

Installation of functional groups onto the aforementioned 90° ligand angle 9H-carbazole-3,6-dicarboxylic acid (H_2cdc)-based cages is considerably more challenging and thus these types of cages have been less widely studied. The first cage of this series, $Cu_{12}(cdc)_{12}$, was synthesized by Zhou and coworkers in 2009[33] and consists of 6 dicopper paddlewheels and 12 9H-carbazole-dicarboxylate ligands. Zhou subsequently reported the Mo^{2+}, Ru^{2+}, and $Ru^{2+/3+}$ analogues of this cage.[17,26] It was some time later that permanent porosity was demonstrated for the copper member of this isostructural family with $Cu_{12}(cdc)_{12}$ displaying a CO_2 accessible BET surface area of 341 m^2/g.[34] We have recently shown with the report of $Cr_{12}(cdc)_{12}$ (SA_{BET} = 1235 m^2/g) that precise solvent exchange and activation can afford high surface areas for these cages.[35] By employing these practices for the $Cu_{12}(cdc)_{12}$ and $Mo_{12}(cdc)_{12}$ cages, we reported BET surface areas of 1108 and 657 m^2/g, respectively. Although these cages display some of the highest surface areas reported for transition metal-based molecular species, their lack of ligand functionalization limits their solubilty in most solvents. Although we reported the alkylation of the 9-position of carbazoledicarboxylic acid, the resulting cobalt and nickel cages had limited BET surface areas of just 126 and 238 m^2/g, respectively. These cages did display significantly increased thermal stability as compared to the previously reported H_2cdc-based cages.[25]

Carbazole-based ligands have also been widely utilized in MOF syntheses, most notably for several members of the PCN- and DUT-families of frameworks.[36–40] PCN-80 features an octa-carboxylate ligand with four carbazole-dicarboxylates bound to the 3,3',5,5' positions of a biphenyl spacer. The ligands for PCN-81 and -82 are both tetra-carboxylate utilizing a phenyl spacer between two trans-carbazole moieties. The phenyl spacer is fully protonated in PCN-81 and decorated with two trans-methoxy groups in PCN-82. DUT-48 and PCN-81 are isomorphous structures utilizing the same ligand however, DUT-48 is more structurally similar to PCN-82 crystallizing in the same space group and adopting an isosymmetric orientation of the carbazole ligands. DUT-46, -49, -50 and -151 are isoreticular to DUT-48 utilizing naphthyl, biphenyl, terphenyl and tetraphenyl spacers, respectively. DUT-75 and -76 use a single carbazole-dicarboxylate ligand with 4-carboxyphenyl (DUT-75) or 4-carboxybiphenyl (DUT-76) N-functionalization. A subset of these materials, most notably PCN-81/DUT-48 and DUT-49, have been rigorously investigated for the promising high-pressure methane storage properties.[35,41,42]

Although both carbazole-based cages and carbazole-based MOFs show incredible promise for gas storage applications, their advancement has been stymied, at least in part, by the relative difficulty in making ligand on a large scale. As compared to isophthalic acid ligands, a wide variety of which are commercially available, there are limited commercial sources of carbazoledicarboxylic acid molecules. Typical synthetic routes to the carbazole-3,6-dicarboxylate ligand include a Friedel-Crafts alkylation type reaction under highly acidic conditions or lithiation followed by CO_2 quenching.[33,34] Both of these synthesis routes require harsh reaction conditions such as dry HCl (g) or *n/t*-BuLi which makes scaling of the ligand somewhat difficult. In 2014, Eddaoudi and coworkers proposed a catalytic approach for the synthesis of H_2cdc which was found to be reasonably scalable with excellent yield.[43] Reaction of 3,6-dibromo-9H-carbazole and $Zn(CN)_2$ in the presence of catalytic amounts of Zn dust, $Zn(OAc)_2$, $Pd_2(dba)_3$, and dppf under an argon atmosphere for 20 h yielded 9H-carbazole-3,6-dicarbonitrile after workup. Treatment of the dinitrile with aqueous base in the presence of CuI for 35 h yields 9H-carbazole-3,6-dicarboxylic acid (H_2cdc) after workup.

In this work we targeted the synthesis of 9H-carbazole-3,6-dicarboxylic acid under air-stable and transition-metal free conditions utilizing a protecting group strategy that could also be used to tune the thermal, solubility, and adsorption properties of resulting coordination cages. Friedel-Crafts acylation of 9H-carbazole to afford 3,6-diacetyl-9H-carbazole proceeds readily at RT in excellent yield. Attempted oxidation of the acetyl groups to carboxylic acids is low yielding and intensive workups are required to obtain pure product. However, installation of a benzyl protecting group to the N-H position to afford 3,6-diacetyl-9-benzyl-carbazole allows for the clean and high yielding synthesis of 9-benzyl-carbazole-3,6-dicarboxylic acid. Deprotection of the benzyl group with free carboxylates proved low yielding. However, after esterification of the carboxylates the benzyl group can be cleaved in moderate to good yields to afford dimethyl 9H-carbazole-3,6-dicarboxylate. This synthesis route affords a functionalized carbazole-dicarboxylate ligand, 9-benzyl-carbazole-3,6-dicarboxylic acid. The copper cage based on this ligand, $Cu_{12}(benzyl\text{-}cdc)_{12}$ displays intriguing gas adsorption properties and thermal stability that is unprecedented for carbazole-based cages.

Experimental Section

Materials and Methods

All reagents were purchased from commercial vendors at 98% purity or higher and used without further purification.

Ligand Synthesis

3,6-diacetyl-9H-carbazole. $AlCl_3$ (23.9 g, 179.4 mmol) and acetyl chloride (21.3 mL, 299 mmol) were suspended in 200 mL DCM and cooled to 0 °C with stirring. Solid 9H-carbazole (10 g, 59.8 mmol) was added portion-wise over 0.5 h. The resulting reaction mixture was warmed to RT and stirred for 3 h. The reaction mixture was poured into 1 L DI H_2O, added to a separatory funnel and the organic layer collected. The aqueous layer was extracted with DCM (3 x 50 mL), the organic fractions combined, dried over anhydrous $MgSO_4$, the solvent removed via rotary evaporation, and the resulting solid collected. (Yield: 14 g, 93 %) ^{1}H NMR (400 MHz, DMSO-d_6) δ = 12.1 (s, 1 H), 9.0 (d, *J* = 1.6 Hz, 2 H), 8.1 (dd, *J* = 1.6, 8.8 Hz, 2 H), 7.6 (d, *J* = 8.4 Hz, 2 H), 2.7 (s, 6H).

3,6-diacetyl-9-benzyl-carbazole. 3,6-diacetyl-9H-carbazole (7 g, 27.8 mmol) was dissolved in 50 mL DMF, to this solution KOH (9.8 g, 174 mmol) was added and the reaction mixture was allowed to stir at RT for 0.5 h. Benzyl bromide (4.8 mL, 41.7 mmol) was added and the mixture continued stirring at RT for 12 h. The reaction mixture was added to 600 mL DI H_2O, precipitated solids were collected via vacuum filtration. (Yield: 8.6 g, 91 %) ^{1}H NMR (400 MHz, DMSO-d_6) δ = 9.1 (d, *J* = 1.4 Hz, 2 H), 8.1 (dd, *J* = 1.7, 8.7 Hz, 2 H), 7.8 (d, *J* = 8.7 Hz, 2 H), 7.3 (m, 5 H), 5.8 (s, 2 H), 2.7 (s, 6 H).

9-benzyl-carbazole-3,6-dicarboxylic acid. 3,6-diacetyl-9-benzyl-carbazole (8.7 g, 25.5 mmol) was suspended in 210 mL 1,4-Dioxane. In a separate flask NaOH (51 g, 1.275 mol) was dissolved in 210 mL DI H_2O and cooled to 0 °C. The flask containing the cooled NaOH (aq) solution was fitted with an addition funnel filled with 21 mL Br_2, which was added dropwise over 0.25 h. The resulting NaOBr (aq) solution was allowed to stir at 0 °C for an additional 0.5 h. The flask containing the carbazole suspension was fitted with an addition funnel filled with the prepared NaOBr (aq) solution, which was added dropwise over 0.5 h. The resulting reaction mixture was heated to 100 °C for 12 h. After cooling to RT the reaction mixture was added to 500 mL saturated Na_2SO_3 (aq) solution. This solution was then acidified to pH = 1, precipitated solids were collected via vacuum filtration. (Yield: 7.5 g, 85 %) ^{1}H NMR (400 MHz, DMSO-d_6) δ = 12.7 (b, 2 H), 8.9 (d, *J* = 1.4 Hz, 2 H), 8.1 (dd, *J* = 1.6, 8.7 Hz, 2 H), 7.8 (d, 8.6 Hz, 2 H), 7.2 (m, 5 H), 5.8 (s, 2 H).

Dimethyl 9-benzyl-carbazole-3,6-dicarboxylate. 9-benzyl-carbazole-3,6-dicarboxylic acid (2.2 g, 6.5 mmol) and K_2CO_3 (3.6 g, 26 mmol) were suspended in 50 mL DMF and stirred at RT for 0.5 h. Iodomethane (2 mL, 32.5 mmol) was added and the reaction mixture heated to 75 °C for 12 h. After cooling to RT the reaction mixture was added to 500 mL DI H_2O, precipitated solids were collected via vacuum filtration. (Yield: 2.2 g, 92 %) ^{1}H NMR (400 MHz, DMSO-d_6) δ = 9.0 (d, *J* = 1.6 Hz, 2 H), 8.1 (dd, *J* = 1.6, 8.6 Hz, 2 H), 7.8 (d, *J* = 8.7 Hz, 2 H), 7.2 (m, 5 H), 5.8 (s, 2 H), 3.9 (s, 6 H).

Dimethyl 9H-carbazole-3,6-dicarboxylate. Dimethyl 9-benzyl-carbazole-3,6-dicarboxylate (3.6 g, 9.6 mmol) was dissolved in 200 mL DCM and stirred at RT. To this solution $AlCl_3$ (7.7 g, 57.6 mmol) was added and the reaction mixture allowed to stir at RT for 4 h. The reaction mixture was added to 1 L DI H_2O, added to a separatory funnel and the organic layer collected. The aqueous layer was extracted with DCM (3 x 150 mL), the organic portions combined, dried over anhydrous $MgSO_4$, the solvent removed via rotary evaporation and the resulting solid collected. (Yield: 1.8 g, 66 %) ^{1}H NMR (400 MHz, DMSO-d_6) δ = 12.1 (s, 1 H), 8.9 (s, 2 H), 8.1 (d, *J* = 8.4 Hz, 2 H), 7.6 (d, *J* = 8.0 Hz, 2 H), 3.9 (s, 6 H).

Cage Synthesis

Cu_{12}(benzyl-cdc)$_{12}$. H_2benzyl-cdc (69.1 mg, 0.2 mmol) and $Cu(NO_3)\cdot 2.5\ H_2O$ (46.5 mg, 0.2 mmol) were placed in 15 mL of DMA and sonicated until dissolved. The solution was heated at 100 °C for 12 h, over the course of which crystals formed. The reaction was removed from heat, allowed to cool, the mother liquor decanted, and the crystals collected. The crystals were washed with MeOH for 12 h, the MeOH was then decanted and replaced for fresh MeOH 5 times after soaking for at least 12 h between solvent exchanges.

Single-crystal X-ray Diffraction

X-ray structural analysis for 3,6-diacetyl-9H-carbazole, 3,6-diacetyl-9-benzyl-carbazole, Dimethyl 9-benzyl-carbazole-3,6-dicarboxylate and Cu_{12}(9-benzyl-cdc)$_{12}$: Crystals were mounted using viscous oil onto a plastic mesh and cooled to the data collection temperature (109 K for Cu_{12}(benzyl-cdc)$_{12}$, 110 K for 3,6-diacetyl-9H-carbazole, and 100 K for 3,6-diacetyl-9-benzyl-carbazole and Dimethyl 9-benzyl-carbazole-3,6-dicarboxylate). Data were collected on a Bruker-AXS APEX II DUO CCD diffractometer with Cu-Kα radiation (λ = 1.54178 Å) focused with Goebel mirrors for Cu_{12}(9-benzyl-cdc)$_{12}$, 3,6-diacetyl-9H-carbazole, and 3,6-diacetyl-9-benzyl-carbazole; and with graphite-monochromated, fine focused Mo-Kα radiation (λ = 0.71073 Å) for Dimethyl 9-benzyl-carbazole-3,6-dicarboxylate. Unit cell parameters were obtained from 36 to 48 data frames, 0.5° ω, from different sections of the Ewald sphere. The unit-cell dimensions, equivalent reflections and systematic absences in the diffraction data are uniquely consistent with $P2_1/c$ for 3,6-diacetyl-9H-carbazole and Dimethyl 9-benzyl-carbazole-3,6-dicarboxylate. No symmetry higher than triclinic was observed for Cu_{12}(9-benzyl-cdc)$_{12}$ and 3,6-diacetyl-9-benzyl-carbazole, and refinement in the centrosymmetric space group option, *P*-1, yielded chemically reasonable and computationally stable results of refinement. The data were treated with multi-scan absorption corrections.[44] Structures were solved using intrinsic phasing methods[45] and refined with full-matrix, least-squares procedures on F^2.[46]

Two symmetry-unique but chemically identical compound molecules were found in the asymmetric units of 3,6-diacetyl-9H-carbazole and 3,6-diacetyl-9-benzyl-carbazole. The compound molecule in Cu_{12}(9-benzyl-cdc)$_{12}$ was located at an inversion center. As in similar cages, the formula reported corresponds only to the atoms that could be reliably located or calculated, in the case of H-atoms. Thus the sum formula is incomplete and derived quantities would be unreliable. Residual electron density, solvent molecules and atoms that cannot be assigned a reasonable model, were treated as diffused electron density using Squeeze.[47] In Cu_{12}(benzyl-cdc)$_{12}$ three benzyl groups and two DMA solvent molecules,

geometrically constrained, were located disordered in two positions with refined site occupancy ratios of 69.6/30.4, 67.8/32.3, 59.5/40.5, 53.3/46.7 and 52.2/47.8, respectively. Three-dimensional rigid bond restraints on anisotropic parameters were applied to Cu_{12}(benzyl-cdc)$_{12}$. Non-hydrogen atoms were refined with anisotropic displacement parameters. H-atoms in Cu_{12}(benzyl-cdc)$_{12}$, methyl H-atoms and one aryl H-atom in 3,6-diacetyl-9-benzyl-carbazole were treated as idealized contributions with geometrically calculated positions and with U_{iso} equal to 1.2-1.5 U_{eq} of the attached carbon atom, all other H-atoms were located from the difference map and refined independently with isotropic parameters. Atomic scattering factors are contained in the SHELXTL program library.[46] The structures have been deposited at the Cambridge Structural Database under the following CCDC deposition numbers: 1992063-1992066.

Gas Adsorption

CO_2 gas adsorption measurements were measured on a Micromeritics TriStar 3000 Surface Area Analyzer. Prior to measurements, samples were considered activated when their outgas rate under static vacuum was ≤ 2 µbar/min. For CO_2 degas screening the sample was heated at the specified temperature under flowing nitrogen. Full BET CO_2 adsorption measurements were carried out with a sample (105.3 mg) that was flow activated at 75 °C.

Results and Discussion

The work reported here was inspired by the ease of synthesis of N-functionalized carbazole-dicarboxylate ligands such as N-alkyl and phenyl carbazoles.[48,49,50] The prototypical first step in these syntheses is N-position functionalization followed by Friedel-Crafts acylation. 3,6-diacetyl-9H-carbazole has been previously synthesized through Friedel-Crafts acylation of 9H-carbazole. This carbazole moiety is easily synthesized and scaled to produce mass quantities for further functionalization. Initial attempts at directly performing a haloform reaction to the diacetyl derivative using both sodium hypochlorite and hypobromite to afford H_2cdc were unsuccessful, with a multitude of side products being formed which required intensive workup to obtain minimal quantities of carbazole-dicarboxylate.

In most functionalized carbazole derivative syntheses, the initial step prior to acylation is typically removal of the N-H proton. We targeted a protecting group strategy to adapt these syntheses for 9-H carbazole ligands. Typical protecting groups include esters, acetyls, tosylates and benzyl groups. Our syntheses required the use of a protecting group that would tolerate highly alkaline conditions, be easily removed, and have the potential to impart tuneable solid-state properties if utilized for cage synthesis prior to deprotection. Both tosylates and benzyl groups would be stable under refluxing alkaline conditions and could impart interesting properties such as solubility or the potential for π-π stacking which would improve cage thermal stability. Typical deprotection of tosylates involves harsh conditions such as *n*- or *t*-butyl lithium,[51] Grignard reagents[52] or triflic acid.[53] Therefore, we sought to utilize the benzyl protecting group which could be easily removed with $AlCl_3$.[54] Deprotonation of 3,6-diacetyl-9H-carbazole and treatment with benzyl bromide at RT allows for the facile and scalable production of 3,6-diacetyl-9-benzyl-carbazole. After installation of the benzyl group the haloform reaction for the synthesis of 9-benzyl-carbazole-3,6-dicarboxylic acid can be cleanly preformed with workup requiring quenching of excess hypobromite followed by acidification. Precipitated solids can be used for further reaction or for cage synthesis without further purification.

Deprotection of benzyl groups with $AlCl_3$ typically occurs rapidly at room temperature at moderate to good yields. Initial attempts at deprotection with free carboxylic acids present on the ligand were low yielding and likely due to coordination of $Al(OH)_3$, which is produced during aqueous workup, to the carboxylate groups. To mitigate this interaction, the carboxylates were esterified with iodomethane and after esterification the deprotection of the benzyl group occurs rapidly and cleanly to produce dimethyl 9H-carbazole-dicarboxylate. This ligand can then be used for Ullman coupling reactions to synthesize the ligands for the PCN- and DUT- series of frameworks or the esters can be easily deprotected in base to give free 9H-carbazole-3,6-dicarboxylic acid to synthesize M_{12}(cdc)$_{12}$ cages.

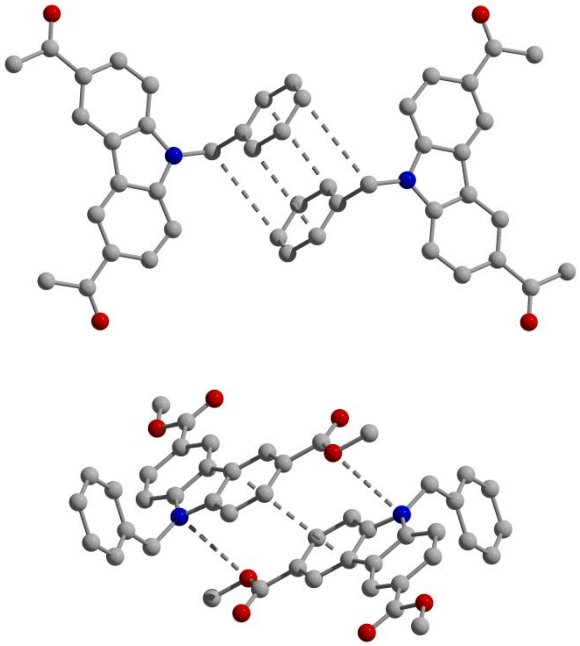

Fig. 2 Packing of ligand precursor molecules in the solid state. The aryl-aryl interactions in 3,6-diacetyl-9-benzyl-carbazole (top) and dimethyl 9-benzyl-carbazole-3,6-dicarboxylate (bottom) of 3.45 to 3.80 Å are expected to endow analogous cages with enhanced cage-cage interactions in the solid state.

Given the lack of reported structures of the ligand intermediates reported here, we sought to characterize the isolated organic intermediates via single-crystal X-ray crystallography. 3,6-diacetyl-9H-carbazole is soluble in a variety of solvents including dichloromethane, tetrahydrofuran, acetone and N,N-dimethylformamide. Dissolution in dichloromethane followed by slow evaporation

of the solvent gave thin colourless plates. The compound crystallizes with H-bonding interactions of 1.99 Å along the c-axis between the N-H of one molecule and the acetyl oxygen of another molecule (see ESI for detailed ligand structure images). 3,6-diacetyl-9-benzyl-carbazole is also highly soluble in a variety of organic solvents and through similar dissolution in dichloromethane followed by slow evaporation of solvent, large colourless block crystals were obtained. This compound crystallizes with a number of π- π interactions among adjacent molecules (Figure 2). There are two carbazole moieties which have benzyl groups in opposing orientations displaying π- π stacking interactions with a distance of 3.77 Å through the carbazole phenyl rings. The benzyl groups of both of these carbazole units have a second π- π interaction with a distance of 4.08 Å to the benzyl group of a third and fourth carbazole molecule. Dimethyl 9-benzyl-carbazole-3,6-dicarboxylate is again highly soluble in a variety of solvents. Dissolution of this material in typical solvents such as dichloromethane followed by solvent evaporation yielded small oily crystals unsuitable for diffraction studies. However, dissolution in minimal quantities of N,N-dimethylformamide followed by slow evaporation of the solvent large colourless block crystals were obtained. The same interactions between the two carbazole moieties as seen in the diacetyl derivative occur in the diester with π- π stacking interactions with a distance of 3.58 Å through the carbazole phenyl rings (Figure 2).

Given the ligand-ligand interactions present in the solid state, coupled with the ease of synthesis of large quantities of benzyl-functionalized ligand, we screened synthetic conditions to isolate octahedral copper cages. As compared to other carboxylate-based ligands, achieving phase purity for these systems is more straightforward as competing phases, including three- and two-dimensional metal-organic frameworks, are rare.[25] Similar to MOF syntheses, we typically screen solvent, co-solvent, reaction temperature, reaction time, pH, and M:L ratio. From a synthetic standpoint, cages have the advantage in that their synthesis is not necessarily coupled to solid crystallization, and more typical molecular recrystallization strategies can be employed to achieve crystalline solid. Ultimately, the reaction of copper(II) nitrate with H_2benzyl-cdc in N,N-dimethylacetamide at 100 °C for 12 h afforded the target compound. As compared to some other functionalized carbazole analogues, H_2benzyl-cdc is highly soluble in amide solvent and rapidly dissolves without heating. Consistent with cage formation being a separate step from solid crystallization, the green metal/ligand solution turns a dark emerald green colour after a few hours of heating with solid crystallization taking place several hours later. After approximately 12 hours, thin plates of Cu_{12}(benzyl-cdc)$_{12}$ are apparent. The crystals remain diffraction quality on the order of days while soaking in their mother liquor, however, given their moderate solubility, they ultimately lose crystallinity if left in amide solvent for extended periods.

Single-crystal X-ray diffraction experiments confirm the compound adopts the expected octahedral structure featuring six dicopper paddlewheel units and 12 carbazole-dicarboxylate ligands (Figures 1,3). The average Cu-Cu distance in the paddlewheels is 2.64 Å and the average cavity distance as measured across the interior Cu positions of the paddlewheel is 13.89 Å. The triangular windows of the cage have an average side length of 11.74 Å as measured between the centroid of adjacent copper paddlewheels. The dicarboxylate ligands bridging the copper paddlewheels flex to form a pinwheel-like structure when viewing down paddlewheels on opposite sides of the cage cavity. The packing diagram of the cages also reveals several π- π interactions as were seen in the ligand structures (Figure 3). Six such interactions occur between adjacent cages with two interactions between the benzyl functional groups and a separate two interactions between the benzyl group of one cage and a carbazole moiety of the adjacent cage. The benzyl-to-benzyl interactions have a distance of 3.96 Å whereas the benzyl-to-carbazole interactions have a distance of 3.92 Å. Cages which share benzyl-to-benzyl interactions are 26.18 Å apart whereas cages which share benzyl-to-carbazole interactions are 21.20 Å apart as measured between the centre of adjacent cages.

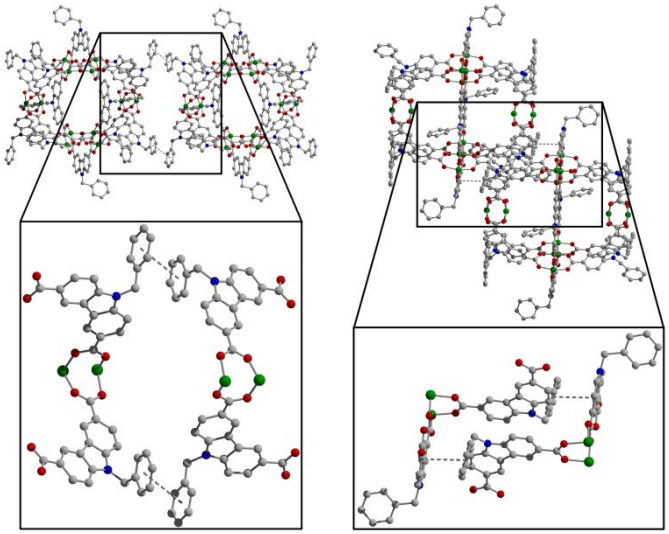

Fig. 3 Solid-state structures for Cu_{12}(benzyl-cdc)$_{12}$ where both benzyl-benzyl (left) and benzyl-carbazole (right) interactions endow the cage with higher surface area and thermal stability as compared to the unfunctionalized Cu_{12}(cdc)$_{12}$ parent cage.

The structural analysis of Cu_{12}(benzyl-cdc)$_{12}$ indicated that the cage may show promise for gas adsorption experiments given its enhanced presence of inter-cage interactions as compared to unfunctionalized Cu_{12}(cdc)$_{12}$. In order to optimize the measured surface area of Cu_{12}(benzyl-cdc)$_{12}$, we screened a wide variety of solvent exchange and activation conditions. That these can have a pronounced effect on porosity is well-known, particularly in the area of metal-organic frameworks. However, for cages solvent exchange and activation conditions are vitally important as their molecular nature can render them incompatible with more typical MOF protocols. For example, it is commonplace in the synthesis and activation of MOFs to perform numerous elevated temperature solvent exchanges with the solvent that was employed in material synthesis to remove any unreacted starting materials and/or

anneal the structure to minimize defects. After this step, subsequent washes with a more volatile solvent are employed to facilitate solvent evacuation during the activation step. Porous molecules are often at least sparingly soluble in their synthesis solvents, precluding the use of many solvents for these washes prior to activation. Indeed, for Cu_{12}(benzyl-cdc)$_{12}$, washing with amide solvent led to the isolation of nonporous samples. To optimize the surface area of this cage, as synthesized sample was isolated by decanting synthesis solvent and washing the material with methanol at room temperature for three days with methanol replaced with fresh solvent five times. Over the course of these washes, the dark green cage sample turned to a pale blue-green colour, indicative of solvent exchange at the copper paddlewheel sites.

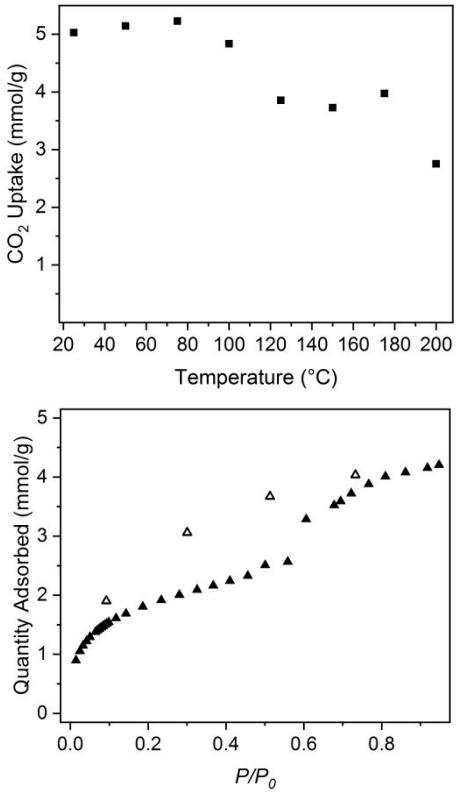

Fig. 4 (Top) Degas survey for Cu_{12}(benzyl-cdc)$_{12}$ where the uptake amount indicated is the amount of CO_2 adsorbed at 0.9 bar and 195 K. (Bottom) Full 195 K CO_2 adsorption isotherm for a sample activated at 348 K.

As compared to metal-organic frameworks, discerning optimal activation conditions for potentially porous cages is also challenging as they are particularly susceptible to phase change as a result of cage rearrangement in the solid state. Thermogravimetric analysis (TGA) is often used to indicate possible optimal activation temperatures for MOFs. The information gleaned from this method, particularly when additional information from differential scanning calorimetry (DSC) is missing, is often over-analysed as phase changes are not apparent with TGA. Accordingly, when targeting optimal activation conditions for a novel cage material, it is important to incrementally survey desolvation temperatures. For Cu_{12}(benzyl-cdc)$_{12}$, preliminary activation of a sample with flowing N_2 at 25 °C gave an N_2 accessible Langmuir surface area of just 44 m^2/g. Given the relatively restricted pore window openings in this structure, it did exhibit a CO_2 accessible Langmuir surface area of 611 m^2/g and pore volume of 0.20 cm^3/g. Activation temperatures were screened in 25 °C increments up to 200 °C. Although 77 K N_2 uptake was considerably lower than 195 K CO_2 uptake across the entire temperature screen, the trends in uptake track fairly well and indicate an optimal activation temperature of 75 °C which resulted in a Langmuir surface area of 924 m^2/g with a pore volume of 0.215 cm^3/g. Notably, this cage displays CO_2 accessible surface area up to an activation temperature of at least 200 °C, in stark contrast to Cu_{12}(cdc)$_{12}$ which is nonporous at an activation temperature of just 100 °C. It is likely that the cage-cage interactions present in the solvated structure of Cu_{12}(benzyl-cdc)$_{12}$ persist, to some extent, upon material activation.

It should be noted that there is considerable complexity in the gas adsorption properties of Cu_{12}(benzyl-cdc)$_{12}$ at some activation temperatures. Namely, at degas temperatures of 50, 75, and 100 °C, there is a considerable step in the 195 K CO_2 uptake. At an activation temperature of 50 °C the amount of gas adsorbed increases form 2.91 mmol/g at 0.4 bar to 3.57 mmol/g at 0.5 bar. A sample heated to 75 °C similarly has a step in its 195 K CO_2 isotherm beginning at 0.4 bar although the magnitude of the step is increased (2.86 to 4.22 mmol/g). Finally, the step for a sample activated at 100 °C is considerably shallower, although the magnitude of the pre- to post-step uptake is similar. For samples activated at all three temperatures, there is considerable hysteresis in the adsorption isotherm that does not close to a desorption pressure of 0.1 bar. Given the discrepancy between pre- and post-step uptake, the BET and Langmuir surface areas of a sample activated at 75 °C are 160 and 712 m^2/g respectively. These surface area values are significantly lower than those calculated for this structure (1265 m^2/g)[55] and reflect significant pore window or surface blockage. It is likely that the benzyl functional groups on the bridging ligands endow the cage with gate-opening type behaviour and are responsible for the step-shaped isotherms. Close inspection of the solvated crystal structure of this cage indicates that 8 of the 12 ligands benzyl groups on the cage are engaged in cage-cage interactions while the remaining four are free to rotate. It is expected that precise tuning of these interactions in extended ligand systems or with mixed-ligand cages can be used to further tailor the uptake properties of these cages for gas storage and separation applications.

Conclusions

The results presented here demonstrate a novel method for the synthesis of benzyl-functionalized carbazole ligand (H_2benzyl-cdc) or unfunctionalized ligand (H_2cdc), an important reagent in the synthesis of a promising class of porous coordination cages. Importantly, our protecting group strategy can be employed to obtain these ligands without the use of

pyrophoric reagents or transition metal-based catalysts. We have further shown that utilization of the benzyl-protected ligand affords a new copper-based octahedral cage, Cu_{12}(benzyl-cdc)$_{12}$ that displays a moderately high surface area and enhanced thermal stability as compared to its unfunctionalized counterpart, Cu_{12}(cdc)$_{12}$. It is our expectation that extension of this strategy to other protecting groups/ligand functional groups is expected to afford new cages with highly tuneable adsorption and thermal properties.

Conflicts of interest

There are no conflicts to declare.

Acknowledgements

This material is based upon work supported by the U.S. Department of Energy's Office of Energy Efficiency and Renewable Energy under the Hydrogen and Fuel Cell Technologies and Vehicle Technologies Offices under Award Number DE-EE0008813. We also thank the Delaware Space Grant College and Fellowship Program, NASA Grant NNX15AI19H, for fellowship support of C.A.R.

References

1 S. S.-Y. Chui, S. M.-F. Lo, J. P. H. Charmant, A. G. Orpen and I. D. Williams, *Science*, 1999, **283**, 1148-1150.
2 H. Li, M. Eddaoudi, M. O'Keeffe and O. M. Yaghi, *Nature*, 1999, **402**, 276-279.
3 N. L. Rosi, J. Kim, M. Eddaoudi, B. Chen, M. O'Keeffe and O. M. Yaghi, *J. Am. Chem. Soc.*, 2005, **127**, 1504-1518.
4 V. Guillerm, L. J. Wesenlinski, Y. Belmabkhout, A. J. Cirns, V. D'Elia, L. Wojtas, K. Adil and M. Eddaoudi, *Nat. Chem.*, 2014, **6**, 673-680.
5 I. M. Honicke, I. Senkovska, V. Bon, I. A. Baburin, N. Bonisch, S. Raschke, J. D. Evans and S. Kaskel, *Angew. Chem. Int. Ed.*, 2018, **57**, 13780-13783.
6 O. K. Farha, I. Eryazici, N. C. Jeong, B. G. Hauser, C. E. Wilmer, A. A. Sarjeant, R. Q. Snurr, S. T. Nguyen, A. O. Yazaydin and J. T. Hupp, *J. Am. Chem. Soc.*, 2012, **134**, 15016-15021.
7 A. C. Sudi, A. R. Millward, N. W. Ockwig, A. P. Cote, J. Kim and O. M. Yaghi, *J. Am. Chem. Soc.*, 2005, **127**, 7110-7118.
8 J. Park, Z. Perry, Y.-P. Chen, J. Bae and H.-C. Zhou, *ACS Appl. Mater. Interfaces*, 2017, **9**, 28064-28068.
9 G. R. Lorzing, B. A. Trump, C. M. Brown and E. D. Bloch, *Chem. Mater.*, 2017, **29**, 8583-8587.
10 J. M. Teo, C. J. Coghlan, J. D. Evans, E. Tsivion, M. Head-Gordon, C. J. Sumby and C. J. Doonan, *Chem. Commun.*, 2016, **52**, 276-279.
11 G. R. Lorzing, E. J. Gosselin, B. A. Trump, A. H. P. York, A. Sturluson, C. A. Rowland, G. P. A. Yap, C. M. Brown, C. M. Simon and E. D. Bloch, *J. Am. Chem. Soc.*, 2019, **141**, 12128-12138.
12 J. Albalad, A. Carne-Sanchez, T. Grancha, L. Hernandez-Lopez and D. Maspoch, *Chem. Commun.*, 2019, **55**, 12785-12788.
13 O. Barreda, G. Bannwart, G. P. A. Yap and E. D. Bloch, *ACS Appl. Mater. Interfaces*, 2018, **10**, 11420-11424.
14 A. Carne-Sanchez, J. Albalad, T. Grancha, I. Imaz, J. Juanhuix, P. Larpent, S. Furukawa and D. Maspoch, *J. Am. Chem. Soc.*, 2019, **141**, 4094-4102.
15 L.-B. Sun, J.-R. Li, W. Lu, Z.-Y. Gu, Z. Luo and H.-C. Zhou, *J. Am. Chem. Soc.*, 2012, **134**, 15923-15928.
16 H. S. M. Coxeter, *Regular Polytopes*, Dover Publications, New York, 1973.
17 J. -R. Li, A. A. Yakovenko, W. Lu, D. J. Timmons, W. Zhuang, D. Yuan and H.-C. Zhou, *J. Am. Chem. Soc.*, 2010, **132**, 17599-17610.
18 Q.-F. Sun, J. Iwasa, D. Ogawa, Y. Ishido, S. Sato, T. Ozeki, Y. Sei, K. Yamaguchi and M. Fujita, *Science*, 2010, **328**, 1144-1147.
19 H. Furukawa, J. Kim, N. W. Ockwig, M. O'Keeffe and O. M. Yaghi, *J. Am. Chem. Soc.*, 2008, **130**, 11650-11661.
20 T.-H. Chen, L. Wang, J. V. Trueblood, V. H. Grassian and S. M. Cohen, *J. Am. Chem. Soc.* 2016, **138**, 9646-9654.
21 D. Fujita, Y. Ueda, S. Sato, N. Mizuno, T. Kumasaka and M. Fujita, *Nature*, 2016, **540**, 563-566.
22 J.-R. Li and H.-C. Zhou, *Nat. Chem.*, 2010, **2**, 893-898.
23 M. Eddaoudi, J. Kim, J. B. Wachter, H. K. Chae, M. O'Keeffe and O. M. Yaghi, *J. Am. Chem. Soc.*, 2001, **123**, 4368-4369.
24 J.-R. Li, A. A. Yakovenko, W. Lu, D. J. Timmons, W. Zhuang, D. Yuan and H.-C. Zhou, *J. Am. Chem. Soc.*, 2010, **132**, 17599-17610.
25 E. J. Gosselin, C. A. Rowland, K. P. Balto, G. P. A. Yap and E. D. Bloch, *Inorg. Chem.*, 2018, **19**, 11847-11850.
26 M. D. Young, Q. Zhang and H.-C. Zhou, *Inorg. Chim. Acta*, 2015, **424**, 216-220.
27 S. Furukawa, N. Horike, M. Kondo, Y. Hijikata, A. Carne Sanchez, P. Larpent, N. Louvain, S. Diring, H. Sato, R. Matsuda, R. Kawano and S. Kitagawa, *Inorg. Chem.*, 2016, **55**, 10843-10846.
28 T.-F. Liu, Y.-P. Chen, A. A. Yakovenko and H.-C. Zhou, *J. Am. Chem. Soc.*, 2012, **134**, 17358-17361.
29 T.-H. Chen, L. Wang, J. V. Trueblood, V. H. Grassian and S. M. Cohen, *J. Am. Chem. Soc.*, 2016, **138**, 9646-9654.
30 D. Zhao, S. Tan, D. Yuan, W. Lu, Y. H. Rezenom, H. Jiang, L.-Q. Wang and H.-C. Zhou, *Adv. Mater.*, 2011, **23**, 90-93.
31 X.-Y. Xie, F. Wu, X. Liu, W.-Q. Tao, Y. Jiang, X.-Q. Liu and L.-B. Sun, *Chem. Commun.*, 2019, **55**, 6177-6180.
32 O. Barreda, G. A. Taggart, C. A. Rowland, G. P. A. Yap and E. D. Bloch, *Chem. Mater.*, 2018, **30**, 3975-3978.
33 J.-R. Li, D. J. Timmons and H.-C. Zhou, *J. Am. Chem. Soc.*, 2009, **131**, 6368-6369.
34 A. Lopez-Olvera, E. Sanchez-Gonzalez, A. Campos-Reales-Pineda, A. Aguilar-Granda, I. A. Ibarra and B. Rodriguez-Molina, *Inorg. Chem. Front.*, 2017, **4**, 56.
35 C. A. Rowland, G. R. Lorzing, E. J. Gosselin, B. A. Trump, G. P. A. Yap, C. M. Brown and E. D. Bloch, *J. Am. Chem. Soc.*, 2018, **140**, 11153-11157.
36 W. Lu, D. Yuan, T. A. Makal, J.-R. Li and H.-C. Zhou, *Angew. Chem. Int. Ed.*, 2012, **51**, 1580-1584.
37 W. Lu, D. Yuan, T. A. Makal, Z. Wei, J.-R. Li and H.-C, Zhou, *Dalton Trans.*, 2013, **42**, 1708-1714.
38 S. Krause, J. D. Evans, V. Bon, I. Senkovska, S. Ehrling, U. Stoeck, P. G. Yot, P. Iacomi, P. Llewellyn, G. Maurin, F.-X. Coudert and S. Kaskel, *J. Phys. Chem. C*, 2018, **122**, 19171-19179.
39 S. Krause, J. D. Evans, V. Bon, I. Senkovska, P. Iacomi, F. Kolbe, S. Ehrling, E. Troschke, J. Getzschmann, D. M. Tobbens, A. Franz, D. Wallacher, P. G. Yot, G. Maurin, E. Brunner, P. L. Llewellyn, F.-. Coudert and S. Kaskel, *Nat. Commun.*, 2019, DOI: 10.1038/s41467-019-11565-3.

40 U. Stoeck, I. Senkovska, V. Bon, S. Krause and S. Kaskel, *Chem. Commun.*, 2015, **51**, 1046-1049.
41 U. Stoeck, S. Krause, V. Bon, I. Senkovska and S. Kaskel, *Chem. Commun.*, 2012, **48**, 10841-10843.
42 S. Krause, V. Bon, I. Senkovska, U. Stoeck, D. Wallacher, D. M. Tobbens, S. Zander, R. S. Pillai, G. Maurin, F.-C. Coudert and S. Kaskel, *Nature*, 2016, **532**, 348-352.
43 L. J. Weselinski, R. Luebke and M. Eddaoudi, *Synthesis*, 2014, **46**, 596-599.
44 Apex3; Bruker AXS Inc.: Madison, WI, 2015.
45 G. M. Sheldrick, *Acta. Cryst.*, 2015, **A71**, 3-8.
46 G. M. Sheldrick, *Acta. Cryst.*, 2015, **C71**, 3-8.
47 A. L. Spek, *Acta. Cryst.*, 2015, **C71**, 9-18.
48 H.-P. Zhou, Y.-M. Zhu, C.-M. Cui, P. Wang, H.-W. Li, J.-Y. Wu, Y. Xie, M.-H. Jiang, X.-T. Tao and Y.-P. Tian, *Inorg. Chem. Commun.*, 2006, **9**, 351-354.
49 X. Jiang, Y. Liu, P. Wu, L. Wang, Q. Wang, G. Zhu, Z.-L. Li and J. Wang, *RSC Adv.*, 2014, **4**, 47357-47360.
50 P. Wu, M. Jiang, Y. Li, Y. Liu and J. Wang, *J. Mater. Chem. A*, 2017, **5**, 7833-7838.
51 E. Alonso, D. J. Ramon and M. Yus, *Tetrahedron*, 1997, **53**, 14355-14368.
52 N. Shohji, T. Kawaji, S. Okamoto, *Org. Lett.*, 2011, **13**, 2626-2629.
53 T. Javorskis and E. Orentas, *J. Org. Chem.*, 2017, **82**, 13423-13439.
54 T. Guney, J. J. Lee and G. A. Kraus, *Org. Lett.*, 2014, **16**, 1124-1127.
55 L. Sarkisov and A. Harrison, Mol. Simul., 2011, 37, 1248-1257.